ELECTRON SPIN RESONANCE SPECTRA OF ORIENTED RADICALS[1]

J. R. MORTON

Division of Applied Chemistry, National Research Council, Ottawa, Canada

Received April 29, 1964

CONTENTS

I. INTRODUCTION

A. SCOPE OF THE REVIEW

It is now well known that paramagnetic fragments (radicals) can be trapped in a crystal matrix. The trapped species may be introduced by doping processes, or by radiation damage of the host crystal, and may be studied by the technique of electron spin resonance. Fortunately, the trapped radicals are almost always oriented; that is, they lie in a limited number of precisely aligned orientations connected by the crystal symmetry.

Recent articles (13, 67) have reviewed the information obtainable from the spectra of randomly trapped radicals and from radicals in solution, and it is the purpose of the present work to discuss the spectra of oriented radicals trapped in single crystals.

A great deal of data has been amassed on the e.s.r. of radiation-damaged organic crystals, mostly the dicarboxylic acids and the amino acids. A review of this subject will be followed by a discussion of paramagnetic fragments trapped by doping or radiation processes in inorganic crystals. With the exception of a short section on oriented triplet-state radicals, attention will be confined to doublet systems, *i.e.*, those possessing a single unpaired electron.

B. THE ELECTRON SPIN RESONANCE METHOD

The theory and practice of electron spin resonance has been extensively treated (38, 104), and the present discussion will be confined to essentials.

An electron has a spin S of $^1/_2$, that is, its spin angular momentum is $^1/_2(h/2\pi)$. The magnetic moment μ_S associated with the spin of electron is given by

$$\mu_S = -g\beta S \qquad \text{(Eq. 1)}$$

where β is the Bohr magneton and g, the magnetogyric ratio of the electron, is equal to 2.0023.

In a homogeneous magnetic field, the component of the spin angular momentum in the field direction is restricted to $\pm^1/_2(h/2\pi)$, allowing a parallel or antiparallel alignment of the spin magnetic moment in the field. The two configurations correspond to the Zee-

(1) N.R.C. No. 8067.

man levels of the unpaired electron, and their energies are $\pm{}^1/_2(g\beta H)$. The resonance condition for a transition between the two Zeeman components is therefore

$$h\nu = g\beta H \qquad \text{(Eq. 2)}$$

where $g = 2.0023$ and $\beta = 1.39967$ Mc./sec./gauss. With a magnetic field of several thousand gauss, the electron spin resonance may be induced by suitably polarized microwave radiation, the Boltzmann distribution of the spins between the two states ensuring a net absorption of the microwave energy. In practice a microwave cavity containing the sample is placed in a homogeneous magnetic field. An e.s.r. spectrometer is essentially a device for supplying microwave power to the cavity and for detecting changes in its Q. The resonance is sought by slowly varying the magnetic field through the value indicated by Eq. 2, and the signal may be displayed either on an oscilloscope or by means of a recording potentiometer.

In general, however, e.s.r. spectra do not consist of a single absorption line, as might appear to be indicated by the above discussion. The detection of many lined spectra leads to the conclusion that the magnetic field H experienced by the unpaired electron is

$$H = H_0 + H' \qquad \text{(Eq. 3)}$$

where H_0 is the field due to the spectrometer magnet and H' is a perturbing field originating in the sample itself. Usually, H' is a measure of the "hyperfine" interaction between the unpaired electron and nearby magnetic nuclei. In the case of a radical trapped in a crystal matrix, H' is anisotropic with respect to the orientation of the crystal in the main magnetic field H_0. For example, the spectrum of OH radicals in γ-irradiated ice crystals at 77°K. varies with the angle between H_0 and the O–H bond (82).

In general, the perturbation H' is tensorial, and the extraction of the component tensor elements and their interpretation is the chief task of the e.s.r. spectroscopist. The tumbling motion undergone by radicals observed in the liquid phase averages the anisotropic part of H' to zero, and analysis of the spectra yields only its trace or isotropic component. On the other hand, it may be difficult to extract the principal elements of the H' tensors from the spectra of radicals trapped in glassy, amorphous, or powdered matrices. This is because all possible radical orientations are present, and the resulting spectra are, except in simple cases, difficult to analyze (3, 113, 124). However, the study of radicals trapped in single crystals can yield both the isotropic and the anisotropic part of H', and the analysis of the spectra is simplified by the exact overlap of the signal from similarly aligned radicals (127, 128).

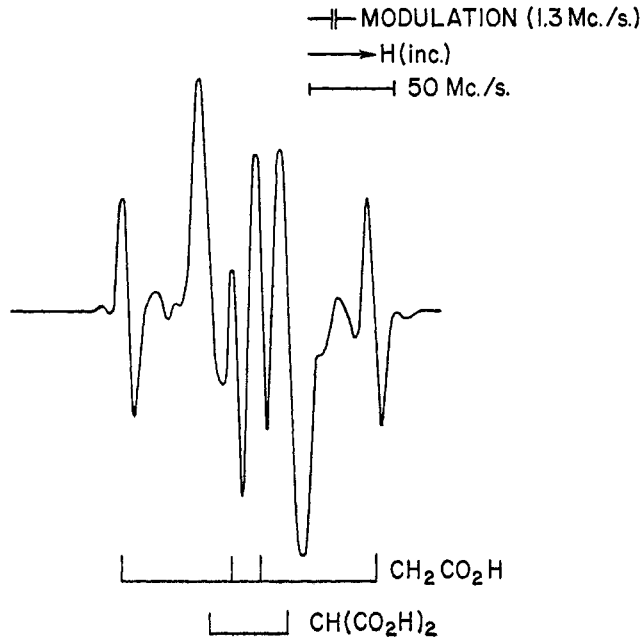

Fig. 1.—First derivative e.s.r. spectrum of $CH(CO_2H)_2$ and $CH_2(CO_2H)$ radicals in γ-irradiated malonic acid.

II. The Electron-Nuclear Hyperfine Interaction

A. General Remarks

The orbital of the unpaired electron in a paramagnetic species will, in general, extend over several of the atoms of which the radical is composed. The interaction between the electron and a nuclear magnetic dipole ($I \geqslant {}^1/_2$) gives rise to the hyperfine splitting commonly encountered in e.s.r. spectra. At sufficiently high magnetic fields, the components of the electron- and nuclear-spin angular momenta in the field direction are definable by M_S and M_I, where $M_S = \pm{}^1/_2$ and M_I can have the $2I + 1$ values between $+I$ and $-I$. The hyperfine interaction energy results in a splitting of the electronic Zeeman levels (defined by M_S) into sublevels defined by M_I. This hyperfine splitting is exhibited by the absorption spectrum, which is governed by the selection rules $\Delta M_S = 1$, $\Delta M_I = 0$.

Hyperfine splittings due to protons are frequently observed in e.s.r. spectra. A single proton ($I = {}^1/_2$) splits each Zeeman level into two sublevels, resulting in a two-line spectrum. Such a spectrum is exhibited by the radical $CH(CO_2H)_2$ in γ-irradiated malonic acid (78). Two protons interacting with the unpaired electron result in a further splitting into a four-line spectrum—for example, the radical $CH_2(CO_2H)$ also trapped in irradiated malonic acid (57). The spectra of both these species are shown in Fig. 1. Three protons give rise to an eight-line spectrum (51, 99), and, in general, the hyperfine interaction of n nuclei of spin-${}^1/_2$ will give rise to a spectrum consisting of 2^n equally intense lines. If two or more *equivalent* spin-${}^1/_2$ nuclei

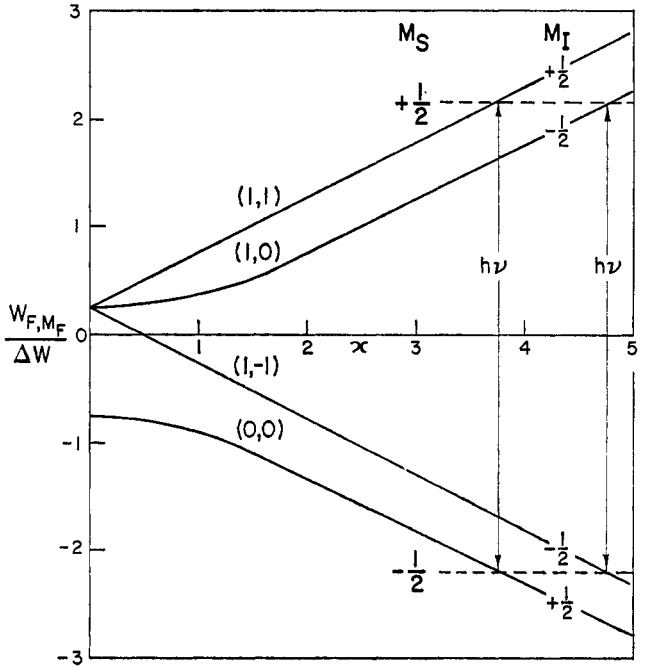

Fig. 2.—Energy level diagram for $S = 1/2$, $I = 1/2$, and the allowed high-field transitions.

interact, superposition of some of the lines results in a spectrum of $n + 1$ lines (to first order) of binomial intensity distribution; for example, the 1:2:1 type of spectrum (74) due to two equivalent fluorine nuclei ($I = 1/2$) exhibited by the radical CF_2CONH_2; the 1:3:3:1 spectrum (48) of the radical $CH_3C(CO_2H)_2$; and the 1:6:15:20:15:6:1 spectrum (60) of the trapped radical $(CH_3)_2C(CO_2H)$.

Commonly encountered nuclei of spin $I = 1$ are N^{14} and the deuteron H^2. Hyperfine interaction with such nuclei contributes to the spectrum a triplet of equally intense, equally spaced (to first order) lines corresponding to the M_I values -1, 0, and $+1$ (66, 87, 94, 95).

B. THE SPIN HAMILTONIAN

An effective spin Hamiltonian describing the interaction between a nucleus and an electron in a magnetic field H_0 is

$$\mathcal{H} = \beta S \cdot \mathbf{g} \cdot H_0 + S \cdot \mathbf{T} \cdot I \qquad \text{(Eq. 4)}$$

The first term represents the energy of interaction of the electronic magnetic moment with the magnetic field, and the second the interaction between the electron and the nucleus. A term involving direct interaction between the nuclei and the magnetic field ($-\gamma H_0 \cdot I$) has been neglected since its effect, which is primarily to relax the selection rule $\Delta M_I = 0$, is rarely encountered at X-band frequencies.

If the orbital angular momentum of the unpaired electron were completely quenched the second-rank tensor **g** would be equal to 2.0023 (the free-spin g-value) times the unit tensor. In other words, **g** would be isotropic and equal to 2.0023, as discussed in section I. However, small deviations from the free-spin g-value have been observed and interpreted (65, 79) in terms of spin-orbit interaction between the ground state and excited states of the radical. The tensor **g** is, however, symmetrical and its principal values are always close to the free-spin g-value.

The second term in Eq. 4 represents the hyperfine interaction between the electronic spin S and the nuclear spin I described by the second-rank tensor **T**. Insofar as **g** is nearly isotropic, the hyperfine tensor **T** will be a symmetrical 3 × 3 matrix which can be diagonalized and resolved into isotropic and anisotropic components. The effective Hamiltonian $\mathcal{H}'$ for the hyperfine interaction energy can be written (1)

$$\mathcal{H}' = (8\pi g\beta\gamma/3)\psi^2(0) S \cdot I - g\beta\gamma[S \cdot I \cdot r^{-3} - 3(S \cdot r)(I \cdot r)r^{-5}] \qquad \text{(Eq. 5)}$$

where γ is the magnetogyric ratio of the interacting nucleus. The eigenvalues of $\mathcal{H}'$ are the principal values of **T**, and the isotropic and anisotropic components of **T** correlate with the first and second terms, respectively, in Eq. 5.

1. *The Isotropic Hyperfine Interaction*

The first term in Eq. 5 gives rise to a nonzero hyperfine splitting only if there is a finite probability of finding the unpaired electron at the interacting nucleus, as indicated by the factor $\psi^2(0)$. For this reason the isotropic interaction is usually called the "contact" or Fermi interaction (36).

In zero field the electronic and nuclear spins couple to form the resultant F such that

$$F_+ = I + 1/2 \quad \text{or} \quad F_- = I - 1/2$$

The two values of F define states between which there is a zero-field splitting of

$$\Delta W = [1/2(2I + 1)]\frac{8\pi}{3} g\beta\gamma\psi^2(0) \qquad \text{(Eq. 6)}$$

In a magnetic field H_0 the spin Hamiltonian including the *isotropic* hyperfine term is

$$\mathcal{H} = \beta S \cdot g \cdot H_0 + \mathbf{A} S \cdot I \qquad \text{(Eq. 7)}$$

where

$$\mathbf{A} = 2\Delta W/(2I + 1) = (8\pi g\beta\gamma/3)\psi^2(0) \qquad \text{(Eq. 8)}$$

The solution to Eq. 7 is (12, 101)

$$W_{F,M_F} = \frac{\Delta W}{2(2I + 1)} \pm \frac{\Delta W}{2}\left(1 + \frac{4M_F x}{2I + 1} + x^2\right)^{1/2} \qquad \text{(Eq. 9)}$$

where $x = g\beta H_0/\Delta W$, and M_F is the magnetic quantum number of F.

The form of the hyperfine interaction is shown in Fig. 2 for the case $I = 1/2$. At low ($x < 0.1$) and intermediate ($x \simeq 1$) magnetic fields, transitions are governed by the selection rules $\Delta F = 0, \pm 1$; $\Delta M_F = 0, \pm 1$. At higher magnetic field strengths ($x > 3$), F and M_F are no longer good quantum numbers. The electronic and nuclear spins precess independently

about H_0 (Paschen–Back effect), and the four energy levels are defined by the quantum numbers M_S and M_I, both of which can be $\pm 1/2$.

$$W_{M_S M_I} = g\beta H_0 M_S + \mathbf{A} M_I M_S \qquad \text{(Eq. 10)}$$

Electron spin resonance transitions between these energy levels are governed by the selection rules $\Delta M_S = \pm 1$, and $\Delta M_I = 0$. The hyperfine interaction constant **A** determines the separation between hyperfine lines corresponding to successive M_I-values.

It will be apparent from Eq. 8 that the *isotropic* hyperfine interaction **A** will only be nonzero if $\psi^2(0)$ is nonzero; that is, if the orbital of the unpaired electron has s-character. In fact, it is possible to estimate the s-character of the orbital of the unpaired electron by comparing the experimentally determined **A** with a parameter $\mathbf{A}_0$ calculated as if the unpaired electron were wholly in the ns-orbital of the nucleus concerned. Values of $\psi^2(0)$ may be computed for s-orbitals of various nuclei using s.c.f. wave functions (19, 85, 122, 123), and multiplication by the factor $(8\pi g\beta\gamma/3h)$ yields the parameters $\mathbf{A}_0$ listed in Table I.

Particularly when the s-character of the orbital of the unpaired electron is small, the significance of the experimental isotropic hyperfine parameter **A** is somewhat reduced because of the possibility of inner-shell polarization (7). However, when the orbital has appreciable s-character, for example, an sp^3-orbital (58), relatively greater significance can be attached to the ratio $\mathbf{A}/\mathbf{A}_0$.

2. *The Anisotropic Hyperfine Interaction*

The second term in Eq. 5 imparts to the effective Hamiltonian $\mathcal{H}'$ an anisotropic or direction-dependent character. The experimentally determinable tensor(s) **T** can be resolved into the isotropic part discussed in the previous section and a traceless, anisotropic part deriving from the second term in Eq. 5. The traceless tensor describes the hyperfine interaction energy consequent upon the classical interaction of the electronic and nuclear dipoles. The anisotropic hyperfine energy is (40, 134)

$$W'_{M_S,M_I} = \frac{g\beta\gamma M_I M_S}{2}\left\langle \frac{1 - 3\cos^2\alpha}{r^3} \right\rangle_{\text{av}} (1 - 3\cos^2\theta) \qquad \text{(Eq. 11)}$$

where r is the distance from the nucleus to the unpaired electron, α is the angle between this line and a principal axis of the tensor, θ the angle between H_0 and the same principal axis. W' clearly represents an anisotropic hyperfine energy, because of the $(1 - 3\cos^2\theta)$ term; on the other hand, W' will only be nonzero if the unpaired electron has p- or d-character, since the value of $\langle (1 - 3\cos^2\alpha) r^{-3} \rangle$ is zero for s-electrons. In fact, it is possible to estimate the p-character of the orbital of the unpaired electron by comparing the observed anisotropic hyperfine splitting **B** with a parameter $\mathbf{B}_0$ obtained from s.c.f. wave functions.

TABLE I

ATOMIC PARAMETERS $\psi^2_{ns}(0)$ AND $\langle r^{-3}\rangle_{np}$ (A.U.) AND ONE-ELECTRON HYPERFINE CONSTANTS (M.C.P.S.)

Nucleus	n	$\psi^2_{ns}(0)$	A_0	$\langle r^{-3}\rangle_{np}$	B_0	Reference
H^1	1		1420			
B^{11}	2	1.408	2020	0.775	53	19, 85, 100
C^{13}		2.767	3110	1.692	91	15, 19, 85
N^{14}		4.770	1540	3.101	48	15, 19, 85
O^{17}		7.638	4628	4.974	144	19, 100
F^{19}		11.966	47910	7.546	1515	19, 27
Si^{29}	3	3.807	3381	2.041	87	100, 122
P^{31}		5.625	10178	3.319	287	15, 122
S^{33}		7.919	2715	4.814	78	15, 122
Cl^{35}		10.643	4664	6.710	137	15, 122
As^{75}	4	12.460	9582	7.111	255	75, 100, 123
Xe^{129}	5	26.71	33030	17.825	1052	85, 97

The hyperfine interaction between an unpaired electron in a p-orbital of an atom and the magnetic nucleus of that atom is usually found to be an axially symmetric tensor of the form $\mathbf{A} + 2\mathbf{B}$ parallel to the p-orbital direction, and $\mathbf{A} - \mathbf{B}$ perpendicular to it. Thus, **A** is the isotropic parameter associated with s-character, and **B** is the anisotropic parameter associated with p-character. An estimate of the p-character of the orbital of the unpaired electron may be obtained by comparing the experimentally determined **B** with a theoretical $\mathbf{B}_0$, where $\mathbf{B}_0 = (2g\beta\gamma/5h)\langle r^{-3}\rangle_{np}$. Values of $\langle r^{-3}\rangle_{np}$ have been computed from available (19, 85, 122, 123) wave functions and are included in Table I together with the corresponding value of $\mathbf{B}_0$.

III. SOME EXPERIMENTAL CONSIDERATIONS

A. THE SPECTROMETER

In an electron spin resonance experiment the sample is placed in a microwave cavity held in a homogeneous magnetic field. The magnetic field is modulated at some frequency usually between 400 c.p.s. (2) and 120 kc.p.s. (10). As a result of an electron spin resonance, microwave power is absorbed by the sample, and the change in the microwave level is detected by a silicon–tungsten crystal. The output from the detector has a component at the modulation frequency, and further amplification at this frequency is carried out with a phase-sensitive detector. In general, sensitivity is higher at higher modulation frequencies because of the "$1/f$" nature of the noise at the crystal detector. Spectrometers operating with modulation frequencies as high as 455 kc.p.s. (72) and 975 kc.p.s. (110) have been described. An alternative technique is that of superheterodyne detection (52, 116). Microwave power reflected from the sample cavity is mixed with that from a local oscillator klystron and detected at an intermediate frequency of 30 Mc.p.s. or higher. In such spectrometers modulation of the magnetic field and final signal amplification can be at a low audio frequency.

Most electron spin resonance spectrometers can easily be adapted to single crystal work. The crystal may be rotated about an axis perpendicular to the magnetic field of the spectrometer with the aid of a single-circle or a two-circle (106) goniometer. The low-loss characteristics of Teflon make it a suitable material for construction of those parts of the goniometer which go inside the cavity. An alternative procedure, of course, is to rotate the magnet about the crystal. However, care must be taken to see that the modulation field rotates with the main magnetic field, since the two must remain parallel at all times. Low frequency modulation coils may be attached to the magnet pole faces, but high frequency modulation coils, which are usually an integral part of the cavity, must rotate with the magnet. Such a device is probably rather more satisfactory than a goniometer for studying samples at liquid nitrogen temperature, although a goniometric device has been described for use at liquid helium temperatures (33).

B. CRYSTALLOGRAPHY

It is a fortunate circumstance that paramagnetic species trapped in a single crystal, whether as a result of doping or radiation damage, occupy a limited number of sites usually obeying the symmetry operations of the host crystal. In general, the spectra from the different sites will not superimpose unless the magnetic field of the spectrometer is parallel to some special direction in the unit cell, such as a unique axis. The tensors describing the hyperfine interactions and g-values of the paramagnetic species should refer to a right-handed, orthogonal axis system xyz and it is usually preferable to identify these axes with crystallographically unique axes, if possible. In the case of triclinic crystals, however, the xyz-axis system is chosen with respect to external features of the crystal (57). If it becomes necessary to compare directions in the xyz-axis system with bond directions in the crystal, the relative orientation of the xyz- and the crystallographic abc-axis systems must be known. For a monoclinic crystal, it is convenient to use either the a^*bc- or abc^*-axis system; no "site-splitting" will occur when the magnetic field is parallel or perpendicular to the two-fold crystallographic b-axis. However, when the magnetic field explores planes containing the b-axis, magnetically distinguishable sites may be apparent. The two sites have opposite signs in the corresponding off-diagonal tensor element (94). The obvious orthogonal set of axes to use in the case of a crystal having orthorhombic symmetry is the abc crystallographic axes. In this case there is usually no site splitting for H_0 parallel to a crystallographic axis, but two sites may be apparent for H_0 perpendicular to a crystallographic axis, and four sites observed for a skew direction such as $(3^{-1/2}, 3^{-1/2}, 3^{-1/2})$. As also in the case of a monoclinic crystal, the spectrum for such a skew orientation is useful in establishing the relative signs of the three off-diagonal elements (96).

In the hexagonal crystals of ice the OH radicals (82) were trapped in six sites with their bonds perpendicular to the unique axis, thus conforming to the symmetry of the host crystal. Paramagnetic centers trapped in cubic crystals of LiF at low temperatures include (69) the radical F_2^- and the nearly linear radical F_3^{-2}. These species are oriented so that their internuclear axes are parallel to the face diagonals of the crystal.

It will be apparent from the above remarks that electron spin resonance in crystals cannot be undertaken without giving some consideration to the crystal structure of the substance under investigation. It is essential to know the crystal symmetry, and desirable to know the space group, unit-cell dimensions, and the number of molecules per unit cell. If the atomic coordinates are known, these can often be correlated with principal tensor directions in order to discover the relative orientation of radicals and host molecules.

C. DETERMINATION OF TENSOR ELEMENTS

The anisotropy of the e.s.r. spectrum of a radical trapped in a single crystal can be described by a symmetrical g-tensor $\mathbf{g}$ and, if hyperfine splitting is apparent, by one or more symmetrical hyperfine interaction tensors $\mathbf{T}$. When the magnetic field explores the xy-plane, the off-diagonal element α_{xy} ($\alpha = g^2$ or t^2) is defined positive or negative according as α has a maximum or a minimum value in the quadrant bounded by H_0 parallel to $+x$ and H_0 parallel to $+y$. If α is plotted against angle θ in the xy-plane (arbitrary zero) then the magnitude of α_{xy} is given by

$$4\alpha_{xy}^2 = A^2 - (\alpha_{xx} - \alpha_{yy})^2 \qquad \text{(Eq. 12)}$$

where A is the *full* amplitude of the sinusoidal curve obtained. The accuracy of α_{xy} can best be gauged by plotting against θ the function

$$f(\theta) = {}^1/_2(\alpha_{xx} + \alpha_{yy}) + {}^1/_2(\alpha_{xx} - \alpha_{yy}) \cos 2\theta + \alpha_{xy} \sin 2\theta \qquad \text{(Eq. 13)}$$

and comparing $f(\theta)$ with the experimental curve. If necessary α_{xy} may then be adjusted to give an improved fit to the experimental points. If magnetically distinguishable sites are apparent when H_0 explores the xy-plane, the two sites correspond to positive and negative signs of α_{xy}, and if more than one off-diagonal element has such a sign duality, then their relative signs must be established. This may be done by comparing the observed spectrum for the orientation $(3^{-1/2}, 3^{-1/2}, 3^{-1/2})$ with the spectra predicted as a result of different relative signs in the off-diagonal elements.

Having established the relative signs of the off-diagonal elements, the tensors are transformed (83) into the diagonalizing axis system in order to extract

the three principal values and their direction cosines referred to the *xyz*-axis system.

Since, in general, the tensors **g** and **T** are not diagonal in the *xyz*-axis system, it is more rigorously correct (42, 53) to plot g^2 and t^2 than it is to plot g and t against θ. The principal values of $\mathbf{g}^2$ and $\mathbf{T}^2$ have the same directions as, and are the squares of, the principal values of **g** and **T**.

IV. The E.S.R. Spectra of Trapped Radicals

A. π-Electron Radicals in Radiation-Damaged Organic Crystals

A considerable literature has accumulated on the subject of the e.s.r. spectra of radiation-damaged organic crystals. Naturally, the work has predominantly covered those materials from which single crystals are easily obtained, and these are the saturated dicarboxylic acids and their salts, the simpler amino acids, and certain unsaturated acids. Analysis of the spectra from radiation-damaged crystals of these materials is primarily concerned with the identification of the trapped radical(s) *via* the interpretation of the proton hyperfine interaction. In certain cases, N^{14} and C^{13} hyperfine interactions have been studied, and it appears that a widening of the field to include the fluoroorganics is beginning (27, 28, 74). Most of the work which will be discussed has been carried out on crystals which were irradiated and examined at room temperature. It appears that in certain cases different radicals are trapped if the crystals are irradiated and examined at liquid nitrogen temperature; and further, subsequent warm-up does not necessarily result in the detection of the same radicals as resulted from room temperature irradiation. More work on this aspect of radiation damage is needed.

One type of radical which is commonly detected at room temperature in radiation-damaged organic crystals is a π-electron radical centered on a carbon atom. In such a radical the unpaired electron occupies what is predominantly a carbon 2p-orbital directed perpendicularly to the plane trigonal skeleton of the radical. Since the C^{12} nucleus has zero spin, the hyperfine splitting of the spectra of π-electron radicals in organic crystals is due to interaction between the unpaired electron and α-protons ($\dot{C}$–H_α) and/or β-protons ($\dot{C}$–C–H_β). Hyperfine interaction with the central atom has been studied in crystals enriched with C^{13} ($I = {}^1/_2$) or in the case of certain nitrogen-centered π-radicals (N^{14}, $I = 1$).

1. *Hyperfine Interaction with α-Protons*

In spite of the fact that an α-proton in a π-electron radical lies in the nodal plane of the orbital of the unpaired electron, an isotropic hyperfine interaction between the proton spin and the electron spin may be inferred from the spectra of such radicals. The isotropic hyperfine interaction observable in the spectra of aromatic radicals in solution (13) and the isotropic component of the proton tensor in radicals of the type HCR_1R_2 trapped in organic solids are now widely held to be due to spin polarization in the C–H bond and the consequent small, negative, spin density at the proton. Thus, in Fig. 3, the unpaired electron in the $2p_z$-orbital of the carbon atom causes (76, 126) spin polarization in the sp^2-bonding orbital. According to Hund's rule of maximum multiplicity, there will be a net positive spin density in the carbon orbital, and a net negative spin density in the hydrogen 1s-orbital in accordance with the Pauli principle. Experimentally, it has been confirmed that the spin density at the α-proton in the radical $HC(CO_2H)_2$ is negative (78), and, by observation of $HC^{13}(CO_2H)_2$ signals (77), that the spin density at the central carbon atom is positive. The isotropic hyperfine interaction of -60 Mc.p.s. determined (78) from the spectra of $CH(CO_2H)_2$ trapped in irradiated malonic acid can be regarded as a typical value for radicals of the type HCR_1R_2. As will be seen from Table II a number of such radicals have been identified, and their isotropic hyperfine interactions are remarkably constant in view of the different nature of the various substituents. The isotropic proton hyperfine interaction (a_H) is proportional to the spin density on the central atom (ρ) according to the now widely accepted equation (76)

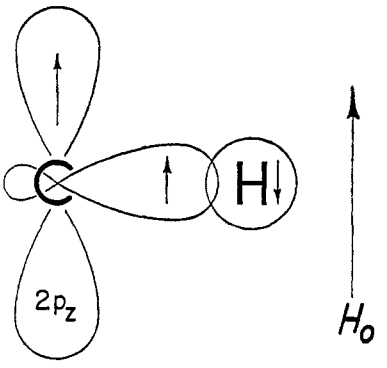

Fig. 3.—Schematic representation of the origin of negative spin density at α-protons.

$$a_H = Q\rho \qquad \text{(Eq. 14)}$$

where Q is a "constant" equal to approximately -60 Mc.p.s.

Also included in Table II are data from the few nitrogen-centered π-radicals known to date. It appears that the isotropic hyperfine interaction of an α-proton in such a radical may be slightly greater than for a carbon-centered radical, but there are insufficient examples to make the evidence conclusive.

It will be apparent from Table II that in addition to the isotropic interaction just discussed, α-protons in trapped π-electron radicals exhibit a characteristic anisotropic interaction. As anticipated in section IIB

TABLE II

HYPERFINE INTERACTIONS WITH α-PROTONS

Radical	Crystal	Hyperfine interaction, Mc.p.s. Isotropic	Anisotropic			Reference
$HC(CO_2H)_2$	$H_2C(CO_2H)_2$	−59	+31	+1	−32	24, 25, 78
$H_2C(CO_2H)$	$H_2C(CO_2H)_2$	−59	+29	+4	−33	57, 59
		−63	+26	+4	−30	
$HCCH_3(CO_2^-)$	$CH_3NH_3^+CH(CO_2^-)$	−54	+30	+6	−36	89, 98
$HCNH_3^+(CO_2^-)$	$NH_3^+CH_2(CO_2^-)$	−62	+35	−5	−30	44, 127
$HCOH(CO_2H)$	$CH_2OH(CO_2H)$	−57	+27	+2	−29	5
$HCF(CONH_2)$	$CH_2F(CONH_2)$	−63	+32	0	−32	28
$HC(CO_2H)$ | $CH_2(CO_2H)$	$CH_2(CO_2H)$ | $CH_2(CO_2H)$	−60	+30	+1	−31	51, 105
$HC(SO_3^-)_2$	$CH_2(SO_3K)_2$	−60	+32	+3	−35	54
$HN^+<$	$(NH_4)_2HPO_4$	−65	+34	+2	−36	94
$HN(SO_3^-)$	$NH_2(SO_3K)$	−64	+39	+4	−43	109

(2), the anisotropic interaction tensor is traceless, and typical principal values are +30, 0, and −30 Mc.p.s. Anisotropic α-proton interactions were first interpreted by Ghosh and Whiffen (44), who studied the radical $HCNH_3^+CO_2^-$ in irradiated glycine, and whose treatment is followed in the present discussion. Consider a planar HCR_2 fragment in which the unpaired electron occupies the carbon 2p π-orbital. Symmetry requires that the three principal directions of the traceless tensor be parallel to the H–C bond, perpendicular to the radical plane, and the mutually perpendicular direction in the plane but perpendicular to the H–C bond. In Fig. 4a the magnetic field H_0 is parallel to the H–C bond, and it will be seen that the unpaired electron density is largely in that volume for which $(1 - 3\cos^2\theta)$ is negative and the hyperfine interaction is positive taking into account the negative magnetic moment of the electron. The +30 Mc.p.s. principal value of the traceless tensor can therefore be associated with the orientation H_0 parallel to the H–C bond. Similarly, in Fig. 4b, where H_0 is in the plane of the

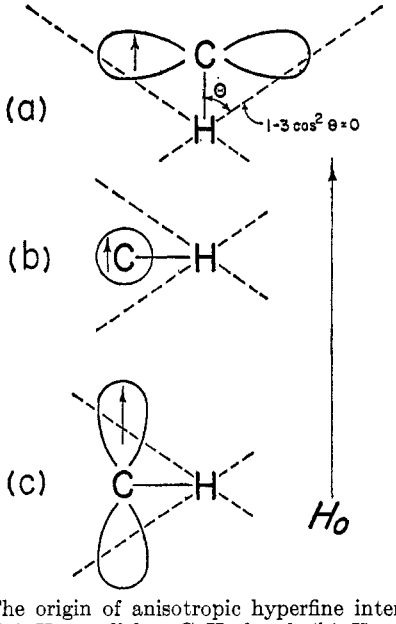

Fig. 4.—The origin of anisotropic hyperfine interaction with α-protons: (a) H_0 parallel to C–H_α bond, (b) H_0 perpendicular to C–H_α and to p-orbital, (c) H_0 perpendicular to radical plane.

radical but perpendicular to the H–C bond, spin density is largely in the region where $(1 - 3\cos^2\theta)$ is positive, and this direction is therefore to be associated with the negative principal value of the hyperfine tensor. Finally, as in Fig. 4c, when H_0 is perpendicular to the radical plane, the average value of $(1 - 3\cos^2\theta)$ will be approximately zero and this direction should be associated with the third (smallest numerically) principal value.

The elucidation of the anisotropic α-proton interaction of the radical $HCNH_3^+CO_2^-$ trapped in irradiated glycine was followed by a similar treatment of the radical $HC(CO_2H)_2$ in irradiated malonic acid (78), and since then by numerous examples, some of which are listed in Table II. The nature of this interaction can by now be regarded as diagnostic of an α-proton in a π-radical, and it has been used to infer radical geometry in a few instances. Thus, the radical $H_2C(CO_2H)$ trapped in irradiated malonic acid (57) contains two α-protons, and from the relative directions of the principal values of their hyperfine tensors it was deduced (a) that the p-orbital direction was perpendicular to both H–C bonds, and (b) that the HCH angle was 116 ± 5°.

Certain features of the geometry of other radicals were deduced by a comparison of the anisotropy of an α-proton interaction with that of β-protons and that of the central atom. Examples will be discussed in the following sections.

2. *Hyperfine Interaction with β-Protons*

The observation of hyperfine interaction between the unpaired electron and both α- and β-protons in the ethyl radical (46) and many other radicals has been rationalized by valence-bond (80) and molecular-orbital (17) calculations. On the one hand, consideration is given to the admixture of states such as

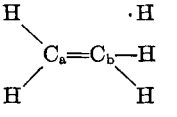

into the ground state of the ethyl radical, and, on the other hand, (hyper)conjugation is invoked between the

TABLE III

ISOTROPIC HYPERFINE INTERACTIONS WITH β-PROTONS (MC.P.S.)

Radical	Crystal	β_1	β_2	β_3	B_2	Reference
$CH_3C(CO_2H)_2$	$CH_3CH(CO_2H)_2$	71	71	71	142	48
$CH_3CH(CO_2^-)$	$CH_3CH(CO_2^-)$ | NH_3^+	70	70	70	140 (300°K.)	88
		120	76	14	122 (77°K.)	56, 89
$CH(CO_2H)$ | $CH_2(CO_2H)$	$CH_2(CO_2H)$ | $CH_2(CO_2H)$	100	80		121	51, 105
$CH(CO_2H)$ | $(CH_2)_3(CO_2H)$	$CH_2CH_2(CO_2H)$ | $CH_2CH_2(CO_2H)$	112	74		127	99
$CH_2C(CO_2H)_2$ | CH_3	$CH_2CH(CO_2H)_2$ | CH_3	70	57		84 or 254	108
$NH_3^+CH(CO_2^-)$	$NH_3^+CH_2(CO_2^-)$	53	53	53	106	44
$N(CH_3)_3^+$	$N(CH_3)_4Cl$	75	75	75	150	117

$2p_z$-orbital of C_α and a pseudo-π-system of the methyl proton group orbitals. In both cases a positive spin density on the methyl protons is predicted, and β-proton interactions are now widely accepted as being of opposite sign to those of α-protons. In contrast to the high anisotropy of α-proton interaction, the interactions of β-protons are almost isotropic. The principal values of the traceless (anisotropic) tensor rarely exceed 10% of the isotropic hyperfine interaction, and for this reason anisotropic components are not included in Table III.

Several radicals are known in which the presence of a methyl group dominates the appearance of the spectrum, contributing three β-protons to the hyperfine pattern. Rotation about the H_3C–C bond renders the three protons equivalent at room temperature, and the methyl group contributes a quartet of intensity 1:3:3:1 and splitting ~70 Mc.p.s. to the spectrum. Three equivalent protons β through a C–N bond have a somewhat smaller hyperfine interaction (53 Mc.p.s.) in the radical $NH_3^+CHCO_2^-$ trapped in irradiated glycine (44).

With the exception of rotating methyl groups it can be seen from Table III that the hyperfine interaction with a β-proton may vary from approximately 14 Mc.p.s. to over 130 Mc.p.s. It appears that methylene groups fixed in the radical can be disinguished by electron spin resonance *via* their different β-proton hyperfine splittings. For example, the spectrum of the radical $(HO_2C)CHCH_2(CO_2H)$ trapped in succinic acid (51, 105) consisted of eight (2^3) lines, demonstrating the distinguishability of the β-protons. The wide range of values of the interaction with β-protons has been interpreted in terms of the variation in angle (θ) between the C_β–H_β bond and the p-orbital direction, projected perpendicular to the C_α–C_β bond. A relationship of the form

$$t_\beta(\theta) = B_0 + B_2 \cos^2\theta \qquad \text{(Eq. 15)}$$

has been suggested (112) where $B_2 >> B_0$, and B_0 may be 0 to +10 Mc.p.s. (56). Thus, in Fig. 5 proton $H_{(1)}$ has a larger interaction (β_1) than that of proton $H_{(2)}$ (β_2) since the projection of C–$H_{(1)}$ is more nearly perpendicular to the radical plane than that of C–$H_{(2)}$. The protons of a rapidly rotating methyl group have a hyperfine interaction of 70 ± 2 Mc.p.s. which appears to be independent of the radical and of the host crystal. Therefore, since

$$\frac{1}{2\pi}\int_0^{2\pi} t_\beta(\theta)\mathrm{d}(\theta) = B_0 + {}^1/_2 B_2 \simeq 70 \text{ Mc.p.s.} \qquad \text{(Eq. 16)}$$

and since B_0 is certainly small and may be zero, B_2 should be approximately 140 Mc.p.s. and independent of the nature of the radical. Values of B_2 have been determined for a number of radicals containing the $-CH_2-$ linkage, and some of these are listed in Table III. With the exception of the radical $CH_3CH_2C(CO_2H)_2$, the B_2-values so obtained are slightly smaller than the anticipated value of 140 Mc.p.s. This may be due to the neglect of a small, positive B_0. The anomalous results obtained from the above radical (108) are not understood.

3. *The Radical CH_3CHR in Irradiated α-Alanine*

Certain results summarized in the previous sections merit discussion in further detail. These concern the radical CH_3CHR (R = CO_2^- or CO_2H) trapped in irradiated α-alanine, $CH_3CH(NH_3^+)CO_2^-$, and the radicals trapped in irradiated glycine, $NH_3^+CH_2$-CO_2^-, to be discussed in the following section.

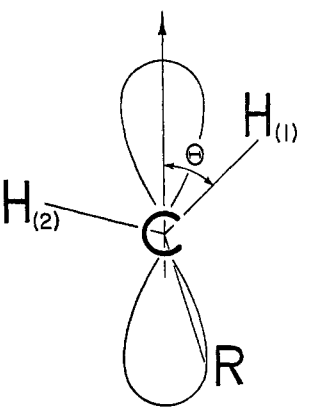

Fig. 5.—Isotropic hyperfine interaction with β-protons.

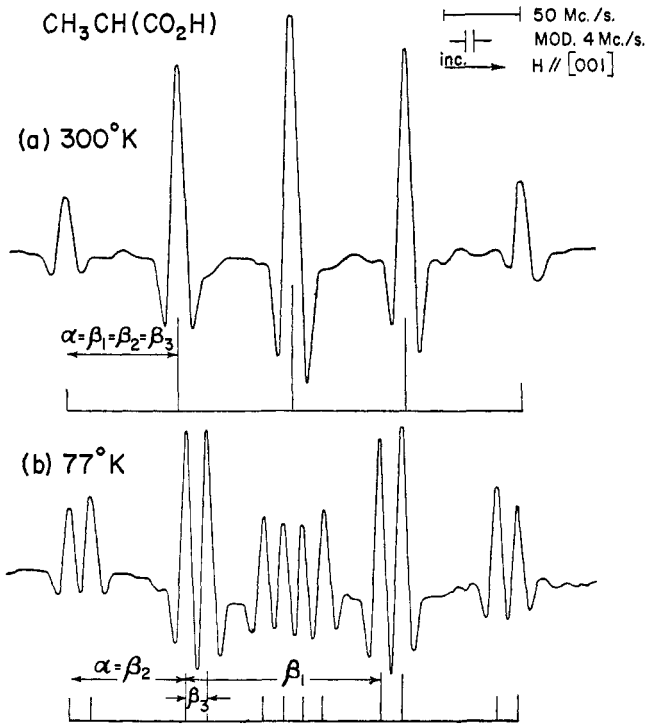

Fig. 6.—Second derivative e.s.r. spectrum of $CH_3CH(CO_2H)$ in γ-irradiated α-alanine at (a) 300°K. and (b) 77°K.

The radical CH_3CHR was first detected in X-irradiated α-alanine by Miyagawa and Gordy (88). They observed and accounted for interesting first-order-forbidden transitions which had appreciable intensity at 24 kMc.p.s. The anisotropy of the spectra has been studied further (98), and it was shown that the three β-protons of the CH_3 group had a slightly larger hyperfine interaction when the magnetic field was parallel to the H_3C–C bond (76 Mc.p.s.) than when it was perpendicular to it (67 Mc.p.s.). This anisotropy, together with the usual α-proton anisotropy, proved that the radical skeleton was planar, and the H_3C–C–H angle was 121 ± 3°.

Interesting changes in the spectra of CH_3CHR have been detected (55, 56, 89) as the host crystal is cooled to 77°K. (Fig. 6). These changes are associated with the slowing down of the methyl group rotation, which at 300°K. is 10^9 c.p.s. or greater, giving the three β-protons equivalent hyperfine interaction of 70 Mc.p.s. At 77°K., the methyl group rotation having slowed to 10^7 c.p.s. or less, the spectra indicate that the three β-protons can be distinguished, and their respective isotropic hyperfine interactions were $\beta_1 = 120$, $\beta_2 = 76$, and $\beta_3 = 14$ Mc.p.s. From these results and eq. 15, it was possible to deduce that $B_0 = +9$, $B_2 = +122$ Mc.p.s.; $\theta_1 = 18$, $\theta_2 = 138$, $\theta_3 = 258°$. In other words the "non-rotating" methyl group has taken up a "skew" configuration with respect to the CCH_α plane of the radical.

At intermediate temperatures (100–200°K.), the transition between the low and the high temperature spectra took place (55, 89). From the broadening of some of the lines of the spectrum, it was possible to estimate the activation energy of the methyl group rotation, a value of approximately 4 kcal. being obtained. This figure must be regarded with caution, however, since it has been shown (48) that in the same, or the very similar, radical CH_3CHCO_2H in methylmalonic acid the methyl group was still rotating at 4°K.

Miyagawa and Itoh (90, 91) have also shown that there is an exchange between hydrogen atoms of the trapped radical and deuterium atoms of the deuterated amino acid host crystal, in the case of irradiated alanine and certain other amino acids. For example, the reaction between the radical CH_3CHR trapped in $CH_3CH(ND_3^+)CO_2^-$ proceeds slowly at room temperature, but at 150° has gone to completion in 1 hr. The final spectrum indicated that the radicals had been fully converted to CD_3CDR. The rate of exchange between the deuterium atoms and an α- or a β-hydrogen atom was equal within the experimental errors. There is no doubt that the exchange does not take place between the amino acid molecules but only between the radicals and the molecules. It will be apparent from these results of Miyagawa and Itoh that caution must be exercised when radicals are identified by means of deuteration studies (*vide infra*).

4. *The Radicals Trapped in Irradiated Glycine*

The spectra of radiation-damaged glycine ($NH_3^+CH_2CO_2^-$) have caused some controversy since the first experiments in 1955 (45). It was variously suggested that the broad triplet which dominates the spectrum of powdered glycine was due to $CH_2NH_3^+$, $CH_2CO_2^-$, or NH_2 (43, 45, 114). It was eventually realized that two radicals were present (118), and Ghosh and Whiffen (43, 44) concluded that they were NH_2 and $NH_3^+CHCO_2^-$. This interpretation was recently challenged by Weiner and Koski (125), who concluded that the radicals were $CH_2CO_2^-$ and NH_4. It was eventually shown (93) that both radicals exhibited C^{13} hyperfine interactions, and that the two radicals were $CH_2CO_2^-$ and $NH_3CHCO_2^-$. It is interesting to ask, however, what were the reasons for the previous misidentifications.

It appears (125) that normal glycine $NH_3^+CH_2CO_2^-$ and D_2-glycine $NH_3^+CD_2CO_2^-$ crystals yield virtually identical spectra, and this observation led to the conclusion that one of the radicals was, not $NH_3^+CHCO_2^-$, but NH_4. The presence of $NH_3^+CHCO_2^-$ in crystals of $NH_3^+CD_2CO_2^-$ can be due only to an exchange of the type discovered by Miyagawa and Itoh in irradiated α-alanine (*vide supra*). Protons of the NH_3^+ group of the host molecules exchange with deuterons of the C–D group of the "initial" radical.

$$\underset{\text{(host crystal)}}{NH_3^+CD_2CO_2^-} + \underset{\text{(initial radical)}}{NH_3^+CDCO_2^-} \rightarrow \underset{\text{(obsd. radical)}}{NH_3^+CHCO_2^-}$$

TABLE IV

CENTRAL ATOM HYPERFINE INTERACTION IN π-ELECTRON RADICALS

Central atom	Radical	Crystal	Hyperfine interaction, Mc.p.s. Isotropic	Anisotropic			Reference
C^{13}	$CH(CO_2H)_2$	$CH_2(CO_2H)_2$	+93	+120	−70	−50	24, 77
	$CH_2(CO_2^-)$	$NH_3^+CH_2(CO_2^-)$	+124	+97	+9	−106	93
	$CHNH_3^+(CO_2^-)$	$NH_3^+CH_2(CO_2^-)$	+127	+127	−60	−37	93
	$CH(SO_3^-)_2$	$CH_2(SO_3K)_2$	+126	+134	−64	−70	54
N^{14}	$N(SO_3^-)_2$	$NH(SO_3K)_2$	+37	+69	−37	−32	54
	$NH^+<$	$(NH_4)_2HPO_4$	+45	+56	−35	−21	94
	$NH(SO_3^-)$	NH_2SO_3K	+38	+60	−32	−28	107
	$NH_2^+(SO_3^-)$	$NH_3^+(SO_3^-)$	+51	+52	−34	−18	109
	NH_3^+	NH_4ClO_4	+55	+7	−1	−6	22, 64

A similar reaction, namely exchange between deuterons of the ND_3^+ group of D_3-glycine and C–H protons of the "initial" radical $CH_2CO_2^-$ to yield the radical $CD_2CO_2^-$, appears to account for Ghosh and Whiffen's observations and their consequent conclusion (43) that this radical was NH_2.

$$\underset{\text{(host crystal)}}{ND_3^+CH_2CO_2^-} + \underset{\text{(initial radical)}}{CH_2CO_2^-} \rightarrow \underset{\text{(obsd. radical)}}{CD_2CO_2^-}$$

5. *Central Atom Hyperfine Interaction in π-Electron Radicals*

In Table IV are listed the isotropic and anisotropic components of C^{13} or N^{14} hyperfine interactions in certain π-electron radicals. The isotropic hyperfine interaction of approximately 120 Mc.p.s. in the case of C^{13}-centered π-radicals and 45 Mc.p.s. for N^{14}-centered π-radicals is a measure of 1s- and 2s-character in the orbital of the unpaired electron. The calculated values of $\mathbf{A}_0$ (Table I) being 3110 and 1540 Mc.p.s. for C^{13} and N^{14}, respectively, it will be seen that even neglecting 1s-polarization, 2s-spin density is only a few per cent. Theoretical treatments of the mechanism of the isotropic interaction between the unpaired electron and the central nucleus in a π-electron radical are available (39, 81).

The anisotropic hyperfine interaction is expected (section IIB) to be of the form $\mathbf{B}_0(3\cos^2\theta - 1)|\rho|$, where ρ is the spin density in the 2p-orbital of the central atom and θ the angle between H_0 and the 2p-orbital density direction. According to Table I, $\mathbf{B}_0$ is 91 Mc.p.s. for C^{13} and 48 Mc.p.s. for N^{14}. The traceless hyperfine interaction tensor should therefore possess axial symmetry, its principal values being $+2\mathbf{B}_0$ parallel to the p-orbital density direction, and $-\mathbf{B}_0$ perpendicular to this direction. The observed central atom hyperfine interaction conforms reasonably well to the expected pattern, and it has been shown for nearly all the examples listed in Table IV, that the largest principal value of the central atom hyperfine interaction is perpendicular to the X–H bond direction determined from the α-proton interaction. The largest principal value of the traceless tensor of the central atom interaction does not attain the expectation value of $2\mathbf{B}_0$ anticipated in Table I, and a 2p-spin density (ρ) of approximately 0.67 would appear to be indicated.

It will be apparent from Table IV that there is deviation (to varying degrees) from the axial symmetry anticipated above in the central-atom interaction. With the exception of NH_3^+ (22), which is tumbling in the lattice at room temperature, the σ-bonds of the central atom are not identical, and it has been suggested (54) that differing spin polarizations in these bonds could account for the loss of axial symmetry. However, calculations indicate (76) that the difference between the two in-plane principal values would not exceed 0.3 Mc.p.s. as a result of such an effect.

Experiments at 77°K. indicate (107, 109) that at this temperature, the anisotropic N^{14} interaction tensor of the radicals $NH(SO_3^-)$ and $NH_2(SO_3^-)$ approaches the axially symmetric form anticipated and that the deviation from axial symmetry at 300°K. is due to hindered rotation of the $-NH_2$ and the $-NH$ group about the S–N bond. The radical $CH_2(CO_2^-)$ in irradiated glycine is also undergoing hindered rotation at 300°K., and low temperature experiments should cause similar changes in the C^{13}-hyperfine interaction.

6. *Radiation Damage in Unsaturated Compounds*

Radicals trapped in the irradiated aliphatic compounds discussed in the previous sections were usually the result of C–H bond rupture, with the formation of a π-orbital consisting primarily of the carbon atom 2p-orbital. It has been shown that the orbital of the unpaired electron in radicals trapped in irradiated olefinic compounds is frequently a *delocalized* π-orbital for example, the allyl-type radical $(HO_2C)CH\cdots CH\cdots CH(CO_2H)$ trapped (50) in irradiated glutaconic acid, $(HO_2C)CH{=}CHCH_2(CO_2H)$. As expected for this type of radical, the spin density on the central carbon atom ($C_{(2)}$) was smaller in magnitude and opposite in sign to that on the adjacent carbon atoms ($C_{(1)}$, $C_{(3)}$). The principal values of the proton hyperfine interaction

tensors were, for $H_{(2)}$ +17, +12, +7 Mc.p.s., and for $H_{(1)}$ and $H_{(3)}$ −53, −36, −18 Mc.p.s.

Another example is that of the radical $(O_2C)CH{=}CH(CO_2^-)$ trapped (49) in irradiated potassium hydrogen maleate, $(HO_2C)CH{=}CH(CO_2^-)K^+$. In this case the unpaired electron occupies a molecular π-orbital extending not only over the two central carbon atoms, but also into the terminal carboxylate groups. The principal values of the proton tensors were −28, −19, and −6 Mc.p.s.

It is interesting to note that on irradiation of fumaric acid (*trans* isomer of maleic acid) a quite different radical was trapped. It appears that a radical $RCH_\beta(CO_2H)CH_\alpha(CO_2H)$ is formed (26), the nature of R being uncertain. Typical hyperfine interactions with H_α and H_β were observed.

Examples are also known of radicals resulting from hydrogen addition at a double bond of the unsaturated compound. Irradiated single crystals of itaconic acid, $CH_2{=}C(CO_2H)CH_2(CO_2H)$, have been shown (41) to contain the radical $CH_3C(CO_2H)CH_2(CO_2H)$, and, in the case of irradiated furoic acid HC=HC—HC=C-(CO₂H), the cyclic radical $H_2C{=}HC{-}HC{=}C(CO_2H)$ is trapped (29). The spectra of the latter radical are also interpreted in terms of a delocalized orbital for the unpaired electron.

7. *g-Tensors of π-Electron Radicals*

The origin of the deviation of the principal g-values in π-electron radicals from the free-spin value 2.0023 is now reasonably well understood (79). The g-shifts are associated with spin-orbit interactions between the ground state and excited states of the radical. If the orbital of the unpaired electron is primarily a carbon $2p_z$-orbital, the competing g-shifts for H_0 perpendicular to z are due to: (a) promotion of a σ(bonding)-electron to pair with the odd electron in the π-orbital, giving a positive g-shift of approximately $2\zeta/\nu_1$ (ζ is the spin-orbit coupling constant); (b) promotion of the odd electron from the π-orbital into an antibonding σ^*-orbital, giving a negative g-shift of approximately $-2\zeta/\nu_2$.

TABLE V

PRINCIPAL VALUES OF g-TENSOR IN π-ELECTRON RADICALS

Radical	Perpendicular to plane (g_{zz})	In plane (g_{xx})	In plane (g_{yy})	Reference
$HC(CO_2H)_2$	2.0026	2.0035	2.0033	78
$H_2C(CO_2H)$	2.0020	2.0042	2.0034	57
$HC(OH)(CO_2H)$	2.0017	2.0053	2.0038	4
$HN^+<$	2.0026	2.0089	2.0048	94
$(O_2C)CH{=}CH(CO_2^-)$	2.0032	2.0052	2.0051	49
$CH_3C(CO_2H)_2$	2.0026	2.0034	2.0044	48

In general the promotion energy ν_2 will exceed ν_1 and so g_{xx} and g_{yy} are expected to be greater than the free-spin g-value. A few typical examples are listed in Table V, and it will be seen that this is the case.

The value of g_{zz} can only be affected by promotion of a σ(bonding)-electron to a σ^*(antibonding)-state. The high frequency of this transition means that g_{zz} will be close to the free-spin g-value, 2.0023, and is expected to be the direction of minimum g for the radical. This prediction is also confirmed by the data in Table V.

B. TRAPPED INORGANIC RADICALS

This section will deal with the somewhat simpler and more symmetric fragments which may be trapped in inorganic crystals either as a result of radiation damage, or by doping processes. Emphasis will be placed on a comparison between isoelectronic species, and on a correlation between the e.s.r. spectral parameters and the anticipated shape and symmetry of the molecule. Where the identification of the radical is dubious, the discussion will be restricted to those results which best correlate with theoretical predictions.

1. *Diatomic Inorganic Radicals*

Table VI lists the principal g-values and, where applicable, principal values of the hyperfine tensors of various diatomic radicals identified by e.s.r. in crystalline matrices. With the exception of F_2^-, XeF, and KrF which are σ-electron radicals, all the species listed are π-electron radicals. This may be inferred from the schematic term scheme of Fig. 7, in which molecular orbitals are constructed from the 2p-orbitals of the separated atoms (not applicable to OH), the crystalline field lifting the degeneracy of the π-orbitals.

Expressions for the principal g-values of trapped diatomic radicals having partially quenched orbital

TABLE VI

PRINCIPAL VALUES OF HYPERFINE INTERACTION (MC.P.S.) AND g-TENSORS OF DIATOMIC RADICALS

Radical	Host crystal		xx	yy	zz[a]	References
N_2^-	KN_3	g	1.984	2.001	2.001	61, 131
		N^{14}	11	11	18	
O_2^+	KCl		2.010	2.042	2.003	66
O_2^-	KCl		1.9512	1.9551	2.4359	70, 71
F_2^-	LiF	g	2.0230	2.0230	2.0031	14, 68, 130
		F^{19}	165	165	2320	
OH	H_2O	g	2.008	2.008	2.013	82
		H^1	99	99	150	
XeF	XeF_4	g	2.1264	2.1264	1.9740	34, 97
		F^{19}	526	526	2637	
		Xe^{129}	1224	1224	2368	
KrF	KrF_4	g	2.068	2.068	2.000	35
		F^{19}	759	759	3531	
$PF^\pm$	NH_4PF_6	g	1.999	(isotropic)		92
		F^{19}	1952	(isotropic)		
		P^{31}	470	(isotropic)		

[a] Interatomic axis.

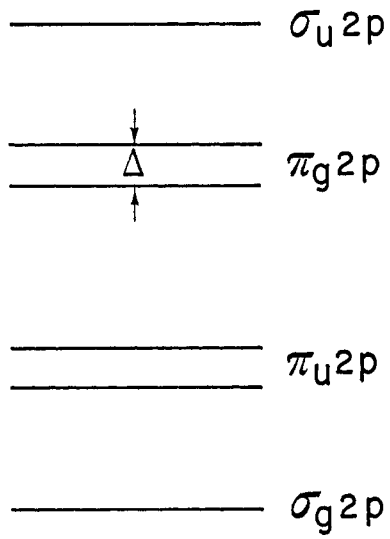

Fig. 7.—Schematic energy-level diagram correlating molecular orbitals of a diatomic molecule with the 2p atomic orbitals.

angular momentum were derived by Kanzig and Cohen (71).

$$g_{zz} = g_0 + 2\left(\frac{\lambda^2}{\lambda^2 + \Delta^2}\right)^{1/2} l, \qquad \text{(Eq. 17)}$$

$$g_{yy} = g_0\left(\frac{\Delta^2}{\lambda^2 + \Delta^2}\right)^{1/2} - \frac{\lambda}{E}\left[+\left(\frac{\lambda^2}{\lambda^2 + \Delta^2}\right)^{1/2} - \left(\frac{\Delta^2}{\lambda^2 + \Delta^2}\right)^{1/2} - 1\right] \qquad \text{(Eq. 18)}$$

$$g_{xx} = g_0\left(\frac{\Delta^2}{\lambda^2 + \Delta^2}\right)^{1/2} - \frac{\lambda}{E}\left[-\left(\frac{\lambda^2}{\lambda^2 + \Delta^2}\right)^{1/2} - \left(\frac{\Delta^2}{\lambda^2 + \Delta^2}\right)^{1/2} + 1\right] \qquad \text{(Eq. 19)}$$

where g_0 is the free-spin g-value 2.0023, l the effective orbital angular momentum about the internuclear axis z, and x the direction of the atomic 2p-orbital. E is the energy separating the states between which there is the spin-orbit interaction. Kanzig and Cohen (70, 71) deduced from the above equations and the data for O_2^- the values $\lambda/\Delta = 0.23$, $\lambda/E = 0.0025$, and $l = 1.04$. For the remaining radicals listed in Table VI (with the possible exception of OH), it may be presumed that orbital angular momentum is quenched ($l = 0$) since $g_{zz} \simeq g_0$ (2.0023). The spin-orbit interaction causes g_{xx} or g_{yy} to deviate from g_0, according to the following rule: if rotation about an axis j belongs to that representation which is the product of the representations of the ground and excited states, then g_{jj} will deviate from 2.0023 as a result of the spin-orbit interaction between the two states. In the group $D_{\infty h}$ (which includes homonuclear diatomic molecules), the operations R_x and R_y (rotation about x and y) belong to the representation Π_g, which is the product of Σ_u and Π_u or of Σ_g and Π_g (129).

Referring to Fig. 7, the positive value of Δg_{yy} in O_2^+ is probably associated with spin-orbit interaction between the states $\sigma_g^1\pi_u^4\pi_g^2$, $^2\Sigma_g$, and $\sigma_g^2\pi_u^4\pi_g^1$, $^2\Pi_g$.

On this basis, however, the isoelectronic radical N_2^- (61, 131) should also have a positive Δg for H_0 perpendicular to the internuclear axis. Possibly the dominating spin-orbit interaction in this case connects the ground-state and an excited state such as $2p\sigma_g^2$-$2p\pi_u^4\,3s\sigma_g^1$, $^2\Sigma_g$.

The radical F_2^- (14, 68, 130) has a $\sigma_g^2\pi_u^4\pi_g^4\sigma_u^1$, $^2\Sigma_u$ ground state, and the positive value of $\Delta g_\perp$ has been associated (20, 65) with spin-orbit interaction between the ground state and the $\sigma_g^2\pi_u^3\pi_g^4\sigma_u^2$, $^2\Pi_u$ excited state. In this case the calculations were carried to second order in λ/E. Similar considerations were applied to the radical XeF (34, 97), although in this case both $^2\Pi$-states ($\sigma^2\pi^{*3}\pi^4\sigma^{*2}$ and $\sigma^2\pi^{*4}\pi^3\sigma^{*2}$) interact with the $^2\Sigma$-ground state. The second-order terms also to some extent account for the negative value of Δg_{zz}.

The hyperfine interaction in the radicals F_2^-, KrF (35), and XeF throws some light on the nature of the antibonding σ-orbital occupied by the unpaired electron. From the data in Table VI it may be calculated that the isotropic hyperfine interaction **A**(F) is 883 Mc.p.s. in F_2^-, 1243 Mc.p.s. in XeF, and 1683 Mc.p.s. in KrF. Compared with $\mathbf{A}_0$(F) = 47,900 Mc.p.s. (Table I), it will be apparent that in each case the isotropic interaction corresponds to a very low spin density in the fluorine 2s-orbital. On the other hand, **B**(F), the anisotropy parameter, may be calculated to be 718, 703, and 924 Mc.p.s. for F_2^-, XeF, and KrF, respectively. Compared to the estimated value of $\mathbf{B}_0$(F) of 1515 Mc.p.s., these figures correspond to a spin density in the F $2p_z$-orbital of 0.47 for F_2^- and XeF, and 0.61 for KrF. From the value for $Xe\langle r^{-3}\rangle_{5p}$ of 17.825 a.u., $\mathbf{B}_0(Xe^{129})$ was calculated to be 1082 Mc.p.s., so that the observed $\mathbf{B}(Xe^{129})$ of 382 Mc.p.s. corresponds to a spin density of approximately 0.36 in the xenon 5p-orbital.

The above discussion reveals that both **A**(F) and **B**(F) are higher for KrF than for XeF. This observation is consistent with those on other isoelectronic sequences (*e.g.*, NO_2, CO_2^-; ClO_3, SO_3^-, PO_3^{-2}) and is associated with higher rare-gas-atom character in the *bonding* orbitals of KrF than in those of XeF, as anticipated by the higher electronegativity of krypton.

The radical $PF^\pm$ has been detected in irradiated crystals of NH_4PF_6 and KPF_6 (92). Unfortunately this radical is tumbling in the lattice at room temperature, and appears to take up random orientations on cooling, so that its anisotropic spectrum has not been elucidated.

2. Triatomic Inorganic Radicals

The triatomic species under consideration are CO_2^- (84, 102, 103) and NO_2 (86, 132, 133), which possess 17 valence electrons; the 19-electron radicals ClO_2 (23) and NO_2^{-2} (66), and the 23-electron radical F_3^{-2} (21). The e.s.r. spectral parameters of these radicals are given

TABLE VII

PRINCIPAL VALUES OF HYPERFINE INTERACTIONS (MC.P.S.) AND g-TENSORS OF TRIATOMIC RADICALS

Radical	No. of e⁻	Host crystal		xx[a]	yy	zz[b]	Reference
CO_2^-	17	HCO_2Na	g	2.0032	1.9975	2.0014	102, 103
			C^{13}	436	422	546	
		$CaCO_3$	g	2.0032	1.9973	2.0016	84
			C^{13}	377	368	497	
NO_2	17	$NaNO_2$	g	2.0057	1.9910	2.0015	133
			N^{14}	138	131	190	
		KNO_3	g	2.0055	1.9932	1.9996	31, 86, 132
			N^{14}	137	141	176	
NO_2^{-2}	19	KCl	g	2.0038	2.0099	2.0070	66[c]
			N^{14}	87	14	20	
ClO_2	19	$KClO_4$	g	2.0036	2.0183	2.0088	23
			Cl^{35}	204	−44	−34	
F_3^{-2}	23	LiF	F^{19}				21
			(central)	715	3146	504	
			(outer)	224	1060	398	

[a] Perpendicular to plane. [b] C_2 axis. [c] Identified as NO in ref. 66.

in Table VII. In this tabulation the xyz-axis system is defined as follows: z is the C_2 axis of the (bent) radicals, x is perpendicular to the radical plane, and y is the mutually perpendicular direction through the terminal atoms. The symmetry operations of bent triatomic molecules (119) are $C_2(z)$, a rotation of 180° about the z-axis, and $\sigma_v(y)$, a reflection in the xz-plane. Type a_1-orbitals are unchanged either by $C_2(z)$ or $\sigma_v(y)$; a_2-orbitals are unchanged by $C_2(z)$ but change sign upon $\sigma_v(y)$; b_1-orbitals change sign upon $C_2(z)$ but are unchanged by $\sigma_v(y)$; and b_2-orbitals change sign upon both symmetry operations.

The operations R_x, R_y, and R_z belong to the representations B_2, B_1, and A_2, respectively (129).

a. The Radicals CO_2^- and NO_2

The valency shell orbitals of AB_2-type molecules have been discussed by Walsh (120) and are tabulated by Ovenall and Whiffen (103) together with an approximate description of the various orbitals. In radicals containing 17 valence electrons, such as CO_2^- and NO_2, the unpaired electron is expected to occupy the totally symmetric $4a_1$-orbital, the ground state being $3b_2^2\,1a_2^2\,4a_1^1$, $^2A_1$. This orbital is primarily a central atom $2p_z$-orbital, but each oxygen $2p_z$-orbital and the carbon 2s-orbital may contribute to it. From the data on CO_2^- it was concluded that the spin density in the carbon $2p_z$-orbital was 0.66 and in the carbon 2s-orbital 0.14. From these figures and Coulson's equations (30), a bond angle of 134° was deduced. It would appear from the more recent calculations (100) summarized in Table I that spin density in carbon $2p_z$ would be better estimated as 0.50. With 0.14 carbon 2s-spin population, a bond angle of approximately 128° is inferred. A similar calculation using the data (133) for NO_2 trapped in $NaNO_2$ at 77°K. yields a bond angle of 135°, in excellent agreement with the value 134° determined for gaseous NO_2 (8).

It will be seen from Table VII that there is a close correlation between the principal g-values of CO_2^- and NO_2. The largest deviation from 2.0023 occurs when the magnetic field of the spectrometer is parallel to the y-axis (the O···O direction). Since R_y belongs to the representation B_1, and the product of A_1 (ground state) and B_1 is B_1, it is states belonging to the representation B_1 which affect Δg_{yy} *via* the spin-orbit interaction. Ovenall and Whiffen concluded that the negative value of Δg_{yy} was due to spin-orbit interaction between the states...$4a_1^0\,2b_1^1$, $^2B_1$ and the ground state...$4a_1^1\,2b_1^0$, $^2A_1$.

The positive value of Δg_{xx} in NO_2 and CO_2^- must be due to interaction between the ground state and a state of b_2 symmetry, most probably...$3b_2^1\,1a_2^2\,4a_1^2$, $^2B_2$.

It appears that the unpaired electron has more central-atom (2s and $2p_z$) character in CO_2^- than in NO_2. This is because, nitrogen being more electronegative than carbon, the inner bonding orbitals will have more central-atom character in NO_2 than in CO_2^-. This trend will be reaffirmed for the series ClO_3, SO_3^-, PO_3^{-2}: in an isoelectronic series of radicals as the electron affinity of an atom X decreases, its share of the *unpaired* electron increases.

b. The Radicals ClO_2 and NO_2^{-2}

These 19-electron radicals are also expected to be bent (120), and gaseous ClO_2 is known to have a bond angle of approximately 117.5° (32). According to Walsh (120) and the tabulation of Ovenall and Whiffen (103) the unpaired electron in ClO_2 and NO_2^{-2} occupies the $2b_1$-orbital, giving the molecule a $^2B_1$ ground state. These radicals are therefore π-electron radicals, the molecular $2b_1$-orbital comprising chlorine $3p_x$- and

oxygen $2p_x$-orbitals directed perpendicular to the radical plane. Cole (23) appears to have assumed that the unpaired electron in ClO_2 occupies an orbital of a_1 symmetry and defined his axis system accordingly. On the basis of the above discussion the principal directions of the Cl^{35} hyperfine interaction tensor and g-tensor of ClO_2 were redefined to conform to the definitions given above. Thus the maximum Cl^{35} hyperfine interaction (204 Mc.p.s.) is assumed in Table VII to define the x-axis, *i.e.*, the perpendicular to the radical plane. With a $...3b_2^2\ 1a_2^2\ 4a_1^2\ 2b_1^1$, $^2B_1$ ground state, Δg_{xx}, is affected by spin-orbit interactions with $^2A_2$ states, Δg_{yy} with $^2A_1$ states, and Δg_{zz} with $^2B_2$ states. The low-lying $...4a_1^1\ 2b_1^2$, $^2A_1$ state is expected to give a large, positive Δg_{yy}, and the principal g-value 2.0183 is therefore assumed to define the y-axis. Smaller, but positive values of Δg_{xx} and Δg_{zz} are also expected and observed as a result of spin-orbit interaction between the ground state and $...3b_2^2\ 1a_2^1\ 4a_1^2\ 2b_1^2$, $^2A_2$ and $...3b_2^1\ 1a_2^2\ 4a_1^2\ 2b_1^2$, $^2B_2$ states, respectively.

The spin population of Cl $3p_z$ in ClO_2 is easily estimated from the anisotropic Cl^{35} hyperfine interaction to be approximately 0.41, so that there is considerable spin density in oxygen $2p_x$-orbitals. There is also a very small positive spin density in the chlorine $3p_y$-orbital.

Jaccard (66) claims to have identified NO_2^{-2} in KCl crystals doped with KNO_2, but comparison of his results with those of Zeldes (132, 133) leads one to suspect that Jaccard's radical is NO_2. On the other hand the radical identified by Jaccard as NO has parameters which could be associated with NO_2^{-2}, by correlation with the data for ClO_2. In agreement with Symons (113), therefore, Table VII gives NO_2^{-2} the parameters ascribed by Jaccard to NO.

c. The Radical F_3^{-2}

This 23-electron radical is formed in LiF crystals X-irradiated at 77°K. and its e.s.r. spectrum may be observed (21) below 40°K. In its ground state such a radical would be expected to be linear (120), the unpaired electron occupying an antibonding, or σ_u-orbital. Somewhat surprisingly, the radical was found to be slightly bent, although this is probably due to environmental effects. More surprising was the postulate that the unpaired electron occupied an a_1-orbital of the (bent) molecule. The isotropic hyperfine interaction with the central nucleus was found to be positive, and it had been concluded that core polarization could yield only a negative isotropic component. The observed isotropic hyperfine interaction was, therefore, thought to be due to admixture of central atom 2s-character into the orbital of the unpaired electron. This possibility could be allowed (by symmetry) only if the unpaired electron occupied an a_1-orbital, and not if it occupied the $b_2(\sigma_u$, if linear)-orbital.

Symons has pointed out (115) that core polarization can and does give rise to positive isotropic hyperfine interactions (*cf.* F_2^-, XeF) and that although large numerically (1500 Mc.p.s.), the central atom isotropic hyperfine interaction is very small compared to $\mathbf{A}_0(F)$, which is estimated (Table I) to be 47,900 Mc.p.s. Assuming, then, that core polarization accounts for the positive isotropic hyperfine interaction, the spectra can be equally well interpreted (115) in terms of a $^2B_2$ ground state, in agreement with the expected electronic configuration in such a molecule.

As will be seen from Table VII, the F^{19} hyperfine interaction tensors deviate somewhat from axial symmetry, the principal values of the anisotropic contribution (along x, y, and z, respectively) being −746, +1649, −903 Mc.p.s. for the central atom and −337, +499, −163 Mc.p.s. for each outer nucleus. These tensors can be written (115) as the sums of pairs of symmetric tensors, the major components corresponding to spin population in the $2p_y$-orbitals of 0.56 for the central atom, and 0.18 for each outer atom, and the minor components to spin populations of approximately 0.04 in $2p_x$ of the central atom and $2p_z$ of the outer atoms.

3. Tetraatomic Inorganic Radicals

In this section radicals derived from the trioxides of the second and third row elements will be discussed. According to Walsh (121), XO_3 molecules possessing 23 valence electrons, such as CO_3^- and NO_3, should be planar with symmetry D_{3h}, whereas the 25-electron radicals NO_3^{-2}, PO_3^{-2}, AsO_3^{-2}, SO_3^-, and ClO_3 will be pyramidal with C_{3v} symmetry.

The unpaired electron in the 23-electron system occupies an a_2'-orbital, which is an out-of-phase combination of the in-plane oxygen lone-pair orbitals. Since there can be no contribution from central atom 2s- or 2p-wave functions to such an orbital, the central atom hyperfine interaction in NO_3 and CO_3^- is zero to first order. As will be seen from Table VIII, a small C^{13} interaction was observed for CO_3^-, but this was probably due to negative spin density in the carbon 1s- or 2s-orbitals as a result of spin polarization in the C–O bonds. It has been suggested (16) that the deviation from axial symmetry in the g-tensors of CO_3^- and NO_3 is due to an in-plane distortion of the molecule giving it effectively C_{2v} symmetry and a $^2B_2$ ground state. Spin-orbit interactions with $^2A_2$ and $^2B_1$ excited states would then account for the positive values of Δg_{zz} and Δg_{yy}, respectively.

The remaining XO_3 radicals listed in Table VIII possess 25 valence electrons and are predicted to be pyramidal with C_{3v} symmetry and a $^2A_1$ ground state. The unpaired electron occupies a totally symmetric a_1-orbital which may assume considerable central atom ns-character.

For example, if the isoelectronic series ClO_3, SO_3^-,

TABLE VIII

PRINCIPAL VALUES OF HYPERFINE INTERACTIONS (MC.P.S.) AND g-TENSORS OF TETRATOMIC RADICALS

Radical	No. of e^-	Host crystal		xx[a]	yy	zz	References
CO_3^-	23	$KHCO_3$	g	2.0066	2.0184	2.0086	16
			C^{13}	−38	−28	−28	
NO_3	23	Urea nitrate	g	2.0066	2.0203	2.0114	16
			N^{14}	<7	<7	<7	
NO_3^{-2}	25	KCl	g	2.0015	2.0057	2.0057	66, 132
		KNO_3	N^{14}	178	89	89	31
PO_3^{-2}	25	$Na_2HPO_3 \cdot 5H_2O$	g	1.9994	2.0011	2.0004	47, 58
			P^{31}	1967	1514	1513	
AsO_3^{-2}	25	$Na_2HAsO_4 \cdot 7H_2O$	g	2.004	2.005	2.005	75
			As^{75}	2033	1590	1590	
SO_3^-	25	$NH_3^+SO_3^-$, etc.	g	2.004	2.004	2.004	15
			S^{33}	428	316	314	
ClO_3	25	NH_4ClO_4	g	2.007	2.008	2.008	22
			Cl^{35}	429	323	323	
HPO_2^-		$NH_4^+H_2PO_2^-$	g	2.0019	2.0035	2.0037	95
			P^{31}	1698	1228	1228	
			H^1	227	238	224	
N_4^-		KN_3	g	2.005	1.997	2.002	111
			Each N^{14}	8	8	26	

[a] In XO_3 molecules, x is perpendicular to O_3 plane.

PO_3^{-2} is considered, Table IX indicates that spin population in the central atom 3s-orbital is approximately 0.1 in each case, but that it increases with decreasing electronegativity of the central atom. Such a trend, already noted for NO_2 and CO_2^- and complemented by the observations on KrF and XeF, is also apparent in the 3p-spin populations listed in Table IX. These observations reflect a decrease (with decreasing electronegativity) in the central atom character of inner bonding orbitals of the molecule, the reduced shielding imparting an increasing central atom character to the orbital occupied by the unpaired electron.

Similar arguments may be applied to the pseudo-isoelectronic series NO_3^{-2}, PO_3^{-2}, AsO_3^{-2}, and the relevant parameters are included in Table IX. The expected increase in central atom character of the orbital of the unpaired electron with decreasing electronegativity of the central atom is apparent, except that $\mathbf{B}/\mathbf{B}_0$ for NO_3^{-2} is too large. This throws further doubt on an already tentative identification (132).

The radical HPO_2^- is of some interest (95) since the proton hyperfine interaction is exceedingly large. This is one of the few examples (another (3) is HCO) of a radical in which there is positive spin density on a proton attached directly to the radical center (an α-proton). In valence bond language, the large proton hyperfine interaction may be due to admixture of a state $H\cdot + \cdot PO_2^-$ with the canonical ground state HPO_2^-. This concept is strengthened by the fact that the radical HPO_2^- reacts with a neighboring $H_2PO_2^-$ ion with the elimination of a H_2 molecule and formation of a dimer-radical $O_2P\text{–}PHO_2$.

TABLE IX

CENTRAL ATOM SPIN POPULATION IN PYRAMIDAL XO_3 RADICALS

	$Cl^{35}O_3$	$S^{33}O_3^-$	$P^{31}O_3^{-2}$	NO_3^{-2}	PO_4^{-2}	AsO_4^{-2}
A[a]	358	353	1665	119	1665	1738
A_0[a]	4664	2715	10,178	1540	10,178	9582
ρ (3s)	0.08	0.13	0.16	0.077	0.16	0.18
B	35	38	152	30	152	148
B_0[a]	137	78	287	48	287	255
ρ (3p)	0.25	0.48	0.53	0.62	0.53	0.57

[a] In Mc.p.s.

Finally, it appears that the radical N_4^- has been detected in ultraviolet-photolyzed potassium azide (111). The radical exhibits hyperfine interaction with four equivalent N^{14} nuclei, and was presumed to be linear (111). However, Symons has suggested (115) that the radical is square-planar.

4. Pentaatomic Inorganic Radicals

The radical PF_4 detected (92) in irradiated NH_4PF_6 presents some interesting features, although, since it is "tumbling" in the crystal lattice at room temperature, it should not be classified as an oriented radical. The spectrum is chiefly notable for the breakdown of the "binomial intensity" rule for equivalent spin-$^1/_2$ nuclei. Thus the spectrum of PF_4 does not consist of a pair of 1:4:6:4:1 quintets, since there is a splitting of the lines of intensity 4 into doublets of intensity 1;3 and also of the line of intensity 6 into a triplet of intensity 1;3,2. Analysis of such second-order splittings in the spectra of transient alkyl radicals has been carried out by Fessenden (37). If I represents the total spin of the equivalent nuclei, with M_I being its component along H_0, the first-order splitting is defined by M_I, and the

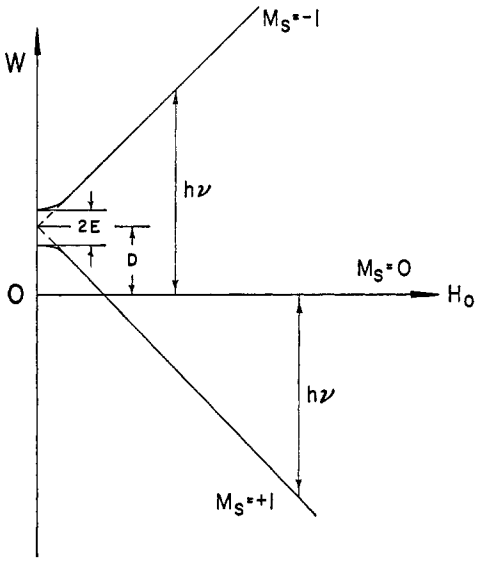

Fig. 8.—Energy level diagram for the triplet state of naphthalene with H_0 perpendicular to the molecular plane.

subsplitting by the values of I available to a particular M_I.

The large P^{31} hyperfine interaction in PF_4 was thought to suggest that the unpaired electron occupied essentially the P 4s-atomic orbital, and if so then this radical is of a similar electronic configuration as NH_4, H_3O, and their derivatives which have been predicted (6, 9) to be thermodynamically stable but have not yet been observed.

C. ORIENTED RADICALS IN THE TRIPLET STATE

1. Phosphorescent Aromatic Molecules

The phosphorescence of organic molecules such as naphthalene is now known to be associated with a metastable triplet state of the molecule, which is reached *via* absorption to an excited singlet state followed by a radiationless transition to the lowest triplet state. The comparatively long lifetime in the triplet state was postulated (73) to be the result of the highly forbidden nature of the triplet → singlet transition to the ground state.

Electron spin resonance spectra of orientated molecules in the triplet state were first observed by Hutchison and Magnum in 1958 (62, 63). Single crystals of durene containing small amounts of the phosphor (naphthalene) were studied at 77°K. while simultaneously populating the triplet state by ultraviolet irradiation. The host crystal had to be (a) transparent to the exciting radiation, and (b) capable of orienting the phosphor molecules. The spin–spin interaction lifts the degeneracy of the three states of the $S = 1$ system, so that even at zero field the energy of the $M_S = 0$ state differs from that of the mean of the $M_S \neq 0$ states by D cm.$^{-1}$. In addition there may be a zero-field splitting between the $M_S \neq 0$ states of $2E$ cm.$^{-1}$. Of course, $|D| > |E|$ and in naphthalene–durene it was found that $D = +0.1003$ cm.$^{-1}$ and $E = -0.0137$ cm.$^{-1}$. In the presence of the magnetic field of the e.s.r. spectrometer the energy of the $M_S = 0$ level is unaffected, whereas the $M_S \neq 0$ levels diverge as in Fig. 8, and may be described as $M_S \pm 1$ states at sufficiently high magnetic fields. The microwave quantum (≃10,000 Mc.p.s., ≃$3D$) is represented by the vertical arrows, the observed transitions corresponding to $\Delta M_S = 1$. The experimental results were described by the Hamiltonian

$$\mathcal{H} = S\cdot\mathbf{T}\cdot S + \beta H_0\cdot\mathbf{g}\cdot S \quad (S = 1) \qquad \text{(Eq. 20)}$$

in which the first term represents the spin–spin interaction described by the second-rank tensor **T**, and the second term represents the interaction of the spin S with the magnetic field H described by the tensor **g**. It was found that **g** was almost isotropic and equal to 2.0030, and the principal values of **T** were $t_{zz} = D$, $t_{yy} = -E$, and $t_{xx} = E$. In this axis system, z is perpendicular to the plane of the naphthalene molecule, and y is parallel to and x perpendicular to the 9,10-carbon atoms of the molecule. These results were incorporated into the simplified Hamiltonian

$$\mathcal{H} = DS_z^2 + E(S_x^2 - S_y^2) + g\beta H_0\cdot S \qquad \text{(Eq. 21)}$$

As indicated in Fig. 8, two transitions were observed, the separation between them being approximately 2150 gauss, $(c/g\beta)|2D|$, for H_0 parallel to z, and 1510 and 630 gauss, $(c/g\beta)[|D| \mp |3E|]$, for H_0 parallel to x and y, respectively.

Proton hyperfine interactions were also apparent in the spectra of the naphthalene triplet, and were consistent with the theory discussed in section IVA1. For example, with H_0 parallel to the x-axis of the naphthalene molecule, the hyperfine interaction of the α-protons will be a maximum, whereas that of the β-protons will be approaching its minimum. Since the α-carbon atoms also have a higher spin density (0.21) than the β-carbon atoms (0.08), the hyperfine quintet observed for H_0 parallel to x was assumed to be due to interaction with the four equivalent α-protons. Successive deuteration at the α-positions confirmed this assignment.

2. Thermally Populated Triplet States

It has been recently shown (18) that ionic single crystals can be prepared containing an anion of the strong π-acceptor tetracyanoquinodimethane (TCNQ), salts such as $Et_3NH^+(TCNQ)_2^-$ and $Ph_3PCH_3^+$-

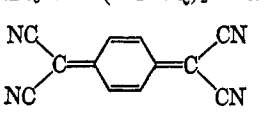

TCNQ

$(TCNQ)_2^-$ being obtained. It appears that in these crystals the radical anions are sufficiently close to

exhibit spin correlation effects characteristic of a singlet ground state and a thermally populated triplet state. As in the case of triplet naphthalene, the three parameters of the Hamiltonian, g, D, and E were determined. For $Ph_3PCH_3^+(TCNQ)_2^-$ and $Ph_3AsCH_3^+(TCNQ)_2^-$, g was almost isotropic and equal to 2.003, $|D|$ was 0.0062 cm.$^{-1}$ (66 gauss), and $|E|$ was 0.00098 cm.$^{-1}$ (10.5 gauss). The rather lower values of $|D|$ and $|E|$ in these salts than in triplet naphthalene presumably reflects the fact that the electrons are constrained to be closer together in naphthalene than in the TCNQ salts.

3. *Ground-State Triplet Molecules*

The electron spin resonance spectrum of oriented diphenylmethylene (C_6H_5–C–C_6H_5) in its ground, triplet state has recently been observed (11). Crystals of benzophenone containing 0.2 mole % diphenyldiazomethane were cooled to 77°K. and irradiated with visible light. Photolysis of the diphenyldiazomethane yielded diphenylmethylene in its ground, triplet state. The parameters of the spin Hamiltonian were $g = 2.0017$, $D = \pm 0.405$ cm.$^{-1}$, and $E = \mp 0.019$ cm.$^{-1}$. Hyperfine interaction with the central C^{13} nucleus was also observed, and was shown to be consistent with the proposed structure (linear C–C^{13}–C), the unpaired electrons occupying orthogonal 2p-orbitals of the central carbon atom.

ACKNOWLEDGMENT.—The author thanks Drs. A. Horsfield and D. H. Whiffen, and Taylor and Francis, Ltd., for permission to reproduce Fig. 1 and 6 from ref. 57 and 56, respectively. Thanks are also extended to the Director of the National Physical Laboratory for permission to use extracts from ref. 100 in Table I. Finally, the author gratefully acknowledges helpful correspondence with D. H. Whiffen, and thanks A. H. Reddoch for his critical perusal of the manuscript.

V. REFERENCES

(1) Abragam, A., and Pryce, M. H. L., *Proc. Roy. Soc.* (London), **A205**, 135 (1951).
(2) Abraham, R. J., Ovenall, D. W., and Whiffen, D. H., *Trans. Faraday Soc.*, **54**, 1128 (1958).
(3) Adrian, F. J., Cochran, E. L., and Bowers, V. A., *J. Chem. Phys.*, **36**, 1661 (1962).
(4) Atherton, N. M., and Whiffen, D. H., *Mol. Phys.*, **3**, 1 (1960).
(5) Atherton, N. M., and Whiffen, D. H., *Mol. Phys.*, **3**, 103 (1960).
(6) Bernstein, H. J., *J. Am. Chem. Soc.*, **85**, 484 (1963).
(7) Bersohn, R., in "Determination of Organic Structures by Physical Methods," Vol. 2, Nachod, F. C., and Phillips, W. D., Ed., Academic Press Inc., New York, N. Y., 1962.
(8) Bird, G. R., *J. Chem. Phys.*, **25**, 1040 (1956).
(9) Bishop, D. M., *J. Chem. Phys.*, **40**, 432 (1964).
(10) Bowers, K. D., Kamper, R. A., and Knight, R. B. D., *J. Sci. Instr.*, **34**, 49 (1957).
(11) Brandon, R. W., Closs, G. L., and Hutchison, C. A., *J. Chem. Phys.*, **37**, 1878 (1962).
(12) Breit, G., and Rabi, I. I., *Phys. Rev.*, **38**, 2082 (1931).
(13) Carrington, A., *Quart. Rev.* (London), **17**, 67 (1963).
(14) Castner, T. G., and Kanzig, W., *J. Phys. Chem. Solids*, **3**, 178 (1957).
(15) Chantry, G. W., Horsfield, A., Morton, J. R., Rowlands, J. R., and Whiffen, D. H., *Mol. Phys.*, **5**, 233 (1962).
(16) Chantry, G. W., Horsfield, A., Morton, J. R., and Whiffen, D. H., *Mol. Phys.*, **5**, 589 (1962).
(17) Chesnut, D. B., *J. Chem. Phys.*, **29**, 43 (1958).
(18) Chesnut, D. B., and Phillips, W. D., *J. Chem. Phys.*, **35**, 1002 (1961).
(19) Clementi, E., Roothaan, C. C. J., and Yoshimine, M., *Phys. Rev.*, **127**, 1618 (1962).
(20) Cohen, M. H., *Phys. Rev.*, **101**, 1432 (1956).
(21) Cohen, M. H., Kanzig, W., and Woodruff, T. O., *J. Phys. Chem. Solids*, **11**, 120 (1959).
(22) Cole, T., *J. Chem. Phys.*, **35**, 1169 (1961).
(23) Cole, T., *Proc. Natl. Acad. Sci.*, **46**, 506 (1960).
(24) Cole, T., and Heller, C., *J. Chem. Phys.*, **34**, 1085 (1961).
(25) Cole, T., Heller, C., and McConnell, H. M., *Proc. Natl. Acad. Sci.*, **45**, 525 (1959).
(26) Cook, R. J., Rowlands, J. R., and Whiffen, D. H., *J. Chem. Soc.*, 3520 (1963).
(27) Cook, R. J., Rowlands, J. R., and Whiffen, D. H., *Proc. Chem. Soc.*, 252 (1962).
(28) Cook, R. J., Rowlands, J. R., and Whiffen, D. H., *Mol. Phys.*, **7**, 31 (1963).
(29) Cook, R. J., Rowlands, J. R., and Whiffen, D. H., *Mol. Phys.*, **7**, 57 (1963).
(30) Coulson, C. A., "Contribution à l'Etude de la Structure Moleculaire," Volume Commémoratif Victor Henri, DeSoer, Liège, 1948, p. 15.
(31) Cunningham, J., McMillan, J. A., Smaller, B., and Yasaitis, E., *J. Phys. Chem. Solids*, **23**, 167 (1962).
(32) Curl, R. F., Heidelberg, R. F., and Kinsey, J. L., *Phys. Rev.*, **125**, 1993 (1962).
(33) Dillon, J. F., Geschwind, S., Jaccarino, V., and Machalett, A., *Rev. Sci. Instr.*, **30**, 559 (1959).
(34) Falconer, W. E., and Morton, J. R., *Proc. Chem. Soc.*, 95 (1963).
(35) Falconer, W. E., Morton, J. R., and Streng, A. G., *J. Chem. Phys.*, in press.
(36) Fermi, E., *Z. Physik*, **60**, 320 (1930).
(37) Fessenden, R. W., *J. Chem. Phys.*, **37**, 747 (1962).
(38) Fraenkel, G. K., in "Physical Methods of Organic Chemistry," Part IV, Weissberger, A., Ed., Interscience Publishers, Inc., New York, N. Y., 1960, Chapter 42.
(39) Fraenkel, G. K., *Pure Appl. Chem.*, **4**, 143 (1962).
(40) Frosch, R. A., and Foley, H. M., *Phys. Rev.*, **88**, 1337 (1952).
(41) Fujimoto, M., *J. Chem. Phys.*, **39**, 846 (1963).
(42) Geusic, J. E., and Brown, L. C., *Phys. Rev.*, **112**, 64 (1958).
(43) Ghosh, D. K., and Whiffen, D. H., *J. Chem. Soc.*, 1869 (1960).
(44) Ghosh, D. K., and Whiffen, D. H., *Mol. Phys.*, **2**, 285 (1959).
(45) Gordy, W., Ard, W. B., and Shields, H., *Proc. Natl. Acad. Sci. U. S.*, **41**, 983 (1955).
(46) Gordy, W., and McCormick, C. G., *J. Am. Chem. Soc.*, **78**, 3244 (1956).
(47) Hanna, M. W., and Altman, L. J., *J. Chem. Phys.*, **36**, 1788 (1962).
(48) Heller, C., *J. Chem. Phys.*, **36**, 175 (1962).
(49) Heller, H. C., and Cole, T., *J. Am. Chem. Soc.*, **84**, 4448 (1962).
(50) Heller, C., and Cole, T., *J. Chem. Phys.*, **37**, 243 (1962).
(51) Heller, C., and McConnell, H. M., *J. Chem. Phys.*, **32**, 1535 (1960).

(52) Hirshon, J. M., and Fraenkel, G. K., *Rev. Sci. Instr.*, **26**, 34 (1955).
(53) Holmberg, R. W., Livingston, R., and Smith, W. T., *J. Chem. Phys.*, **33**, 541 (1960).
(54) Horsfield, A., Morton, J. R., Rowlands, J. R., and Whiffen, D. H., *Mol. Phys.*, **5**, 241 (1962).
(55) Horsfield, A., Morton, J. R., and Whiffen, D. H., *Mol. Phys.*, **5**, 115 (1962).
(56) Horsfield, A., Morton, J. R., and Whiffen, D. H., *Mol. Phys.*, **4**, 425 (1961).
(57) Horsfield, A., Morton, J. R., and Whiffen, D. H., *Mol. Phys.*, **4**, 327 (1961).
(58) Horsfield, A., Morton, J. R., and Whiffen, D. H., *Mol. Phys.*, **4**, 475 (1961).
(59) Horsfield, A., Morton, J. R., and Whiffen, D. H., *Nature*, **189**, 481 (1961).
(60) Horsfield, A., Morton, J. R., and Whiffen, D. H., *Trans. Faraday Soc.*, **57**, 1657 (1961).
(61) Horst, R. B., Anderson, J. H., and Milligan, D. E., *J. Phys. Chem. Solids*, **23**, 157 (1962).
(62) Hutchison, C. A., and Mangum, B. W., *J. Chem. Phys.*, **29**, 952 (1958).
(63) Hutchison, C. A., and Mangum, B. W., *J. Chem. Phys.*, **34**, 908 (1961).
(64) Hyde, J. S., and Freeman, E. S., *J. Phys. Chem.*, **65**, 1636 (1961).
(65) Inui, T., Harasawa, S., and Obata, Y., *J. Phys. Soc. Japan*, **11**, 612 (1956).
(66) Jaccard, C., *Phys. Rev.*, **124**, 60 (1961).
(67) Jen, C. K., in "Formation and Trapping of Free Radicals," Bass, A. M., and Broide, H. P., Ed., Academic Press, New York and London, 1960, Chapter 7.
(68) Kanzig, W., *J. Phys. Chem. Solids*, **17**, 80 (1960).
(69) Kanzig, W., *J. Phys. Chem. Solids*, **17**, 88 (1960).
(70) Kanzig, W., *J. Phys. Chem. Solids*, **23**, 479 (1962).
(71) Kanzig, W., and Cohen, M. H., *Phys. Rev. Letters*, **3**, 509 (1959).
(72) Kawamura, H., and Ishiwatari, K., *J. Phys. Soc. Japan*, **13**, 574 (1958).
(73) Lewis, G. N., and Kasha, M., *J. Am. Chem. Soc.*, **66**, 2100 (1944).
(74) Lontz, R. J., and Gordy, W., *J. Chem. Phys.*, **37**, 1357 (1962).
(75) Lin, W. C., and McDowell, C. A., *Mol. Phys.*, **7**, 223 (1964).
(76) McConnell, H. M., and Chesnut, D. B., *J. Chem. Phys.*, **28**, 107 (1958).
(77) McConnell, H. M., and Fessenden, R. W., *J. Chem. Phys.*, **31**, 1688 (1959).
(78) McConnell, H. M., Heller, C., Cole, T., and Fessenden, R. W., *J. Am. Chem. Soc.*, **82**, 766 (1960).
(79) McConnell, H. M., and Robertson, R. E., *J. Phys. Chem.*, **61**, 1018 (1957).
(80) McLachlan, A. D., *Mol. Phys.*, **1**, 233 (1958).
(81) McLachlan, A. D., Dearman, H. H., and Lefebvre, R., *J. Chem. Phys.*, **33**, 65 (1960).
(82) McMillan, J. A., Matheson, M. S., and Smaller, B., *J. Chem. Phys.*, **33**, 609 (1960).
(83) Margenau, H., and Murphy, G. M., "The Mathematics of Physics and Chemistry," D. van Nostrand Co., Inc., Princeton, N. J., 1956, p. 324.
(84) Marshall, S. A., Reinberg, A. R., Serway, R., and Hodges, J. A., *Mol. Phys.*, in press.
(85) Mayers, D. F., private communication.
(86) Mergerian, D., and Marshall, S. A., *Phys. Rev.*, **127**, 2015 (1962).
(87) Miyagawa, I., and Gordy, W., *J. Chem. Phys.*, **30**, 1590 (1959).
(88) Miyagawa, I., and Gordy, W., *J. Chem. Phys.*, **32**, 255 (1960).
(89) Miyagawa, I., and Itoh, K., *J. Chem. Phys.*, **36**, 2157 (1962).
(90) Miyagawa, I., and Itoh, K., Proceedings of the Symposium on Molecular Structure and Spectroscopy, Tokyo, Sept., 1962.
(91) Miyagawa, I., and Itoh, K., *J. Chem. Phys.*, **40**, 3328 (1964).
(92) Morton, J. R., *Can. J. Phys.*, **41**, 706 (1963).
(93) Morton, J. R., *J. Am. Chem. Soc.*, **86**, 2325 (1964).
(94) Morton, J. R., *J. Phys. Chem. Solids*, **24**, 209 (1963).
(95) Morton, J. R., *Mol. Phys.*, **5**, 217 (1962).
(96) Morton, J. R., *Mol. Phys.*, **6**, 193 (1963).
(97) Morton, J. R., and Falconer, W. E., *J. Chem. Phys.*, **39**, 427 (1963).
(98) Morton, J. R., and Horsfield, A., *J. Chem. Phys.*, **35**, 1142 (1961).
(99) Morton, J. R., and Horsfield, A., *Mol. Phys.*, **4**, 219 (1961).
(100) Morton, J. R., Rowlands, J. R., and Whiffen, D. H., National Physical Laboratory Report No. BPR13, extracted with permission of Director.
(101) Nafe, J. E., and Nelson, E. B., *Phys. Rev.*, **73**, 718 (1948).
(102) Ovenall, D. W., and Whiffen, D. H., *Proc. Chem. Soc.*, 420, 1960.
(103) Ovenall, D. W., and Whiffen, D. H., *Mol. Phys.*, **4**, 135 (1961).
(104) Pake, G. E., "Paramagnetic Resonance," W. A. Benjamin, Inc., New York, N. Y., 1962.
(105) Pooley, D., and Whiffen, D. H., *Mol. Phys.*, **4**, 81 (1961).
(106) Roberts, G., and Derbyshire, W., *J. Sci. Instr.*, **38**, 511 (1961).
(107) Rowlands, J. R., *Mol. Phys.*, **5**, 565 (1962).
(108) Rowlands, J. R., and Whiffen, D. H., *Mol. Phys.*, **4**, 349 (1961).
(109) Rowlands, J. R., and Whiffen, D. H., *Nature*, **193**, 61 (1962).
(110) Semenov, A. G., and Bubnov, N. N., *Instr. Exptl. Tech.* (USSR) (English Transl.), **1**, 96 (1959).
(111) Shuskus, A. J., Young, C. G., Gilliam, O. R., and Levy, P. W., *J. Chem. Phys.*, **33**, 622 (1960).
(112) Stone, E. W., and Maki, A. H., *J. Chem. Phys.*, **37**, 1326 (1962).
(113) Symons, M. C. R., Advances in Chemistry Series, No. 36, American Chemical Society, Washington, D. C., 1962, p. 76.
(114) Symons, M. C. R., *J. Chem. Soc.*, 277 (1959).
(115) Symons, M. C. R., *J. Chem. Soc.*, 570 (1963).
(116) Teaney, D. T., Klein, M. P., and Portis, A. M., *Rev. Sci. Instr.*, **32**, 721 (1961).
(117) Tench, A. J., *J. Chem. Phys.*, **38**, 593 (1963).
(118) Uebersfeld, J., and Erb, E., *Compt. rend.*, **242**, 478 (1956).
(119) Walsh, A. D., *J. Chem. Soc.*, 2260 (1953).
(120) Walsh, A. D., *J. Chem. Soc.*, 2266 (1953).
(121) Walsh, A. D., *J. Chem. Soc.*, 2301 (1953).
(122) Watson, R. E., and Freeman, A. J., *Phys. Rev.*, **123**, 521 (1961).
(123) Watson, R. E., and Freeman, A. J., *Phys. Rev.*, **124**, 1117 (1961).
(124) Weil, J. A., and Hecht, H. G., *J. Chem. Phys.*, **38**, 281 (1963).
(125) Weiner, R. F., and Koski, W. S., *J. Am. Chem. Soc.*, **85**, 873 (1963).
(126) Weissman, S. I., *J. Chem. Phys.*, **25**, 890 (1956).
(127) Whiffen, D. H., in "Free Radicals in Biological Systems," Blois, M. S., Ed., Academic Press, New York, N. Y., 1961, p. 227.

(128) Whiffen, D. H., in "Proceedings Xth Colloquium Spectroscopium International," Lippincott, E. R., and Margoshes, M., Ed., Spartan Books, Washington, D. C., 1963, p. 719.
(129) Wilson, E. B., Jr., Decius, J. C., and Cross, P. C., "Molecular Vibrations," McGraw-Hill Book Co., New York, N. Y., 1955, Appendix X.
(130) Woodruff, T. O., and Kanzig, W., *J. Phys. Chem. Solids*, **5**, 268 (1958).
(131) Wylie, D. W., Shuskus, A. J., Young, C. G., Gilliam, O. R., and Levy, P. W., *Phys. Rev.*, **125**, 451 (1962).
(132) Zeldes, H., in "Paramagnetic Resonance," Vol. II, Low, W., Ed., Academic Press, New York, N. Y., 1963, p. 764.
(133) Zeldes, H., and Livingston, R., *J. Chem. Phys.*, **35**, 563 (1961).
(134) Zeldes, H., Trammell, G. T., Livingston, R., and Holmberg, R. W., *J. Chem. Phys.*, **32**, 618 (1960).